Article

Identification of C_{21} Steroidal Glycosides from *Gymnema sylvestre* (Retz.) and Evaluation of Their Glucose Uptake Activities

Meiyu Liu [1], Tongxi Zhou [2], Jinyan Zhang [1], Guangfeng Liao [1], Rumei Lu [1,*] and Xinzhou Yang [2,*]

[1]   School of Pharmaceutical Sciences, Guangxi University of Chinese Medicine, Nanning 530200, China; lmy13263808041@163.com (M.L.); 18435166743@163.com (J.Z.); guangfengliao@126.com (G.L.)

[2]   School of Pharmaceutical Sciences, South-Central University for Nationalities, Wuhan 430074, China; tc13627123095@163.com

*   Correspondence: lurm@gxtcmu.edu.cn (R.L.); xzyang@mail.scuec.edu.cn (X.Y.); Tel.: +86-0771-4953-513 (R.L.); Fax: +86-27-6784-1196 (X.Y.)

Abstract: *Gymnema sylvestre* (Retz.) Schult is a multi-purpose traditional medicine that has long been used for the treatment of various diseases. To discover the potential bioactive composition of *G. sylvestre*, a chemical investigation was thus performed. In this research, four new C_{21} steroidal glycosides sylvepregosides A-D (**1–4**) were isolated along with four known compounds, gymnepregoside H (**5**), deacetylkidjoladinin (**6**), gymnepregoside G (**7**) and gymnepregoside I (**8**), from the ethyl acetate fraction of *G. sylvestre*. The structures of the new compounds were established by extensive 1D and 2D nuclear magnetic resonance (NMR) spectra with mass spectroscopy data. Compounds **1–6** promoted glucose uptake by the range of 1.10- to 2.37-fold, respectively. Compound **1** showed the most potent glucose uptake, with 1.37-fold enhancement. Further study showed that compounds **1** and **5** could promote GLUT-4 fusion with the plasma membrane in L6 cells. The result attained in this study indicated that the separation and characterization of these compounds play an important role in the research and development of new anti-diabetic drugs and pharmaceutical industry.

Keywords: *Gymnema sylvestre*; C_{21} steroidal glycosides; glucose uptake; GLUT-4

1. Introduction

Diabetes mellitus (DM) is a disease caused by lack of insulin secretion or insulin resistance, which cause the body to experience persistent hyperglycemia and long-term metabolic disorders. DM is classified into type 1 diabetes mellitus (T1DM) and type 2 diabetes mellitus (T2DM), in which T2DM accounts for nearly 95% of individuals, and the number of patients is increasing year by year [1,2]. Insulin resistance (IR) is one of the essential conditions in the development of type 2 diabetes mellitus, and insulin reduces blood sugar levels and improves IR by promoting glucose absorption [3]. Traditional Chinese medicine has used natural products (NPs), including TCM formulations and their extracts, to treat human diseases for thousands of years. Many Chinese herbal medicines and their active ingredients have anti-diabetic properties with minimal side effects, and are widely used in the treatment of T2DM [4]. Therefore, it is of great significance to screen new effective hypoglycemic drugs from natural products through glucose uptake.

Gymnema sylvestre (Retz.) Schult is a genus of tropical plants belonging family Apocynaceae, and mainly distributed in Guangxi, Guangdong, Yunnan, Fujian and Zhejiang provinces of China [5]. *G. sylvestre* was used as a natural remedy for over two millennia. As a traditional Chinese herbal medicine, *G. sylvestre* has the effects of detumescence, fever removal, detoxification, promoting muscle growth, reducing swelling, dispelling wind and relieving pain, and is used to treat diseases such as vasculitis, snake bites, rheumatism, waist and knee pain, etc. [6,7]. Furthermore, *G. sylvestre* has also demonstrated other

important uses, such as hypolipidemic, antiviral, diuretic, antiallergic and antibiotic uses, as well as use as a weight loss supplement [8]. In addition, *G. sylvestre* is also a traditional Chinese ethnic medicine used by Zhuang, Yao, Miao and other ethnic minorities for a long time. Zhuang medicinal ancient books has recorded that *G. sylvestre* has obvious effects in treating diabetes [9]. *G. sylvestre* is widely used as a naturopathic treatment for diabetes. Modern pharmacological studies have found that *G. sylvestre* leaf, root and stem extracts all have hypoglycemic effect [10–12]. Previous studies of this plant afforded that it has broad biological activities for anti-diabetic effect, for example, by suppressing elevated glucose levels in blood, recovering pancreatic beta cells and increasing insulin sensitivity to treat type 2 diabetes mellitus in the earliest stage of disease [13–16]. The serum levels of GLUT-4, PPAR-γ, adiponectin, and leptin have a positive correlation with insulin sensitivity. Study shows that methanolic leaf extract of *G. sylvestre* (MLGS) could upregulate the expression of GLUT-4, PPAR-γ, adiponectin, and leptin, thereby exerting a potent insulin-sensitizing effect [17]. In recent studies, it was also shown that gymnemic acids (GA) separated from *G. sylvestre* (Retz.) Schult decreased blood lipid levels and increased insulin activity in experiments using murine models [18]. The hypoglycemic mechanisms of GA may be related to promoting insulin signal transduction and activating PI3K/Akt- and AMPK-mediated signaling pathways in T2DM rats [19]. Apart from these, GA has the potential for inhibiting electrogenic glucose uptake in the gastrointestinal tract by inhibiting sodium-dependent glucose transporter 1 [20]. Conduritol A is also considered to be the active ingredient in hypoglycemic activity of *G. sylvestre*. Experimental results in rats showed that conduritol A can significantly reduce blood glucose levels and increase blood insulin levels. The hypoglycemic mechanism may be related to improving insulin sensitivity, scavenging free radicals, promoting liver glycogen synthesis, enhancing antioxidant capacity and enhancing immune function [21]. The main components found in *G. sylvestre* are saponins, polysaccharides, sterols, terpenoids, flavonoids, peptides, pectin and so on [22]. Aiming to enhance understanding of the chemical and more anti-diabetic activities constituent of *G. sylvestre*, we performed purification of the EtOAc fraction of the traditional herb, which led to four new C_{21} steroidal glycosides sylvepregosides A-D (**1–4**), together with four known: gymnepregoside H (**5**), deacetylkidjoladinin (**6**), gymnepregoside G (**7**) and gymnepregoside I (**8**) (Figure 1). In addition, compounds **1–6** have effects on increasing glucose uptake in vitro. Compounds **1** and **5** showed a strong glucose uptake in L6 cells, with enhancements up to 2.37- and 1.96-fold. Herein we described the isolation, structure elucidation, the glucose uptake activities as well as the GLUT-4 fusion with the plasma membrane of these isolated compounds.
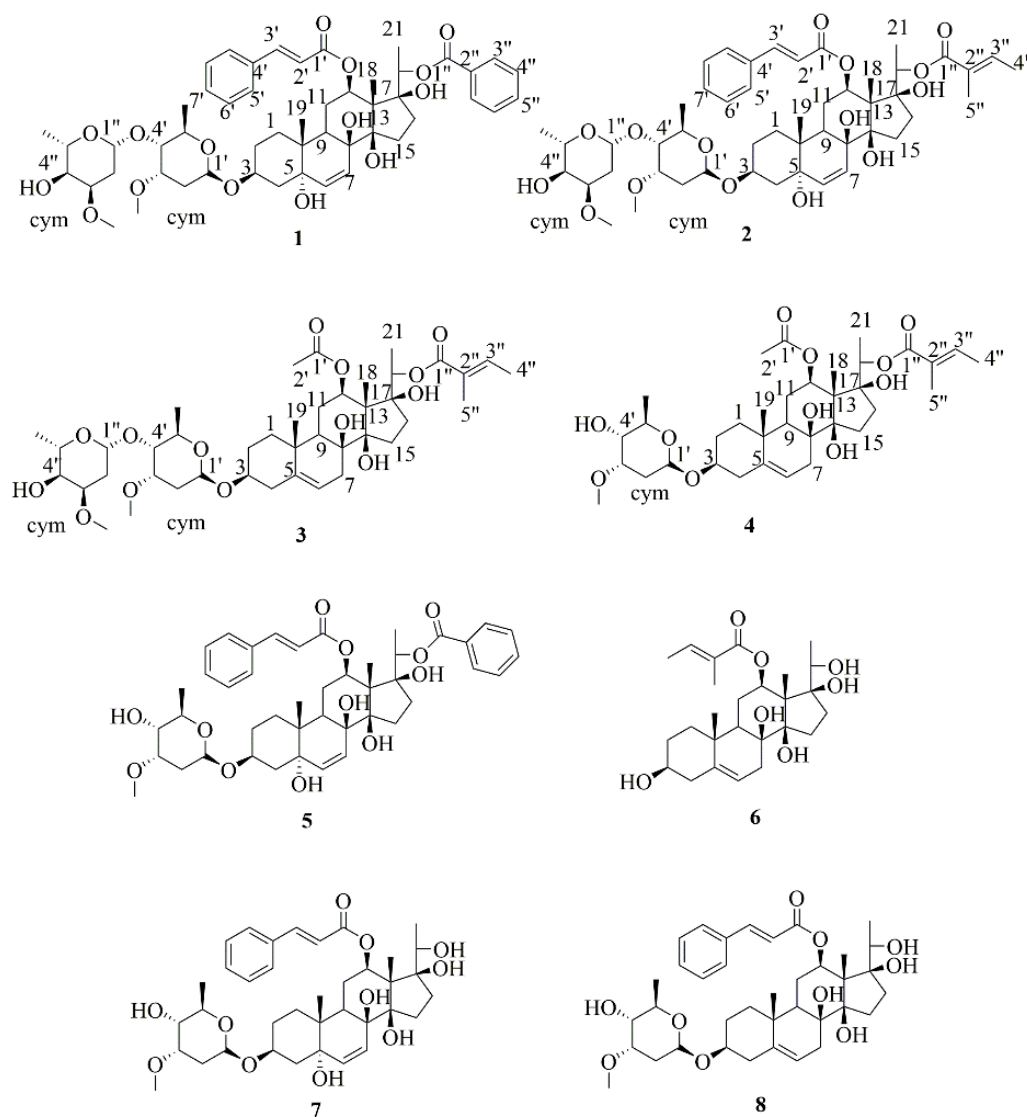
Figure 1. The structures of compounds **1**–**8**.

2. Results and Discussion

Compound **1** was isolated as a white powder. The molecular formula was established as $C_{51}H_{68}O_{15}$ by HRESIMS data (*m/z* 943.4423 [M + Na]$^+$, calcd for 943.4450) (Figure S1, Supplementary Materials). The IR spectrum (Figure S12) showed the characteristic of hydroxyl (3480 cm^{-1}), ester (1713 and 1281 cm^{-1}), and olefinic (1640 cm^{-1}) groups. The ^{1}H and ^{13}C nmR spectra (Table 1) of **1** showed the characteristic signals for the aglycone of C_{21} steroidal glycosides isolated from *Gymnema aliemifoliu* [23], with two angular methyl groups CH$_3$-18 and CH$_3$-19 (δ_H 1.60, 1.01; δ_C 11.5, 21.1), a secondary methyl group CH$_3$-21 (δ_H 1.35; δ_C 15.4), a double bond (δ_{H-6} 5.63 and δ_{H-7} 5.83; δ_C 136.7, 126.3), three oxygenated tertiary carbons, CH-3, CH-12, and CH-20 (δ_H 4.07~4.10, 4.74~4.77, and 4.84; δ_C 74.9, 74.8, and 74.7), and five quaternary carbons, C-5, C-8, C-10, C-14, and C-17 (δ_C 74.6, 74.3, 39.2, 87.5 and 87.8). The above signals the establishment of the 3,5,8,12,14,17,20-heptahydroxypregnane skeleton [24,25], which was further confirmed by detailed analyses of its HSQC, ^{1}H-^{1}H COSY and HMBC spectra (Figures S5–S7). In addition, a cinnamoyl group [δ_H 6.07 and 7.42 (eatch 1H, d, *J* = 16.0 Hz, H-2' and H-3'), δ_H 7.24 (2H, d, *J* = 7.3 Hz, H-5',9'), 7.30~7.36 (5H, m, H-6', 7', 8'); δ_C 166.6, 118.9, 144.3, 134.4, 128.3, 128.5, and 130.2] and a *O*-benzoyl group [δ_H 7.92 (2H, d, *J* = 7.2 Hz, H-3'', 7''), 7.30~7.36 (5H, m, H-4'', 6'') and 7.53 (1H, t, *J* = 7.4 Hz, H-5''); δ_C 165.0, 130.4, 129.9, 128.7 and 133.1] were observed in ^{1}H and ^{13}C nmR spectrum. The HMBC correlations between H-12 (δ_H 4.74~4.77) and C-1'

(δ_C 166.6); between H-20 (δ_H 4.84) and C-1'' (δ_C 165.0) revealed the placement of the two ester groups at C-12 and C-20. The ^{1}H nmR spectrum of **1** showed two anomeric proton signals at δ_H 4.81 (1H, dd, *J* = 9.7, 1.6 Hz) and 4.67 (1H, dd, *J* = 9.7, 1.6 Hz), corresponding to carbon resonances at δ_C 97.7, and 99.5 confirmed by HSQC, and the coupling constants of anomeric proton revealed the sugars were *β*-linkage. The structures of saccharides were determined by analysis of nmR data, including HSQC, ^{1}H-^{1}H COSY, HMBC, NOESY and 1D/2D TOCSY experiments (Figures S5–S10), and further confirmed by comparison of the data with those in the literature [26]. Thus two monosaccharide units were both characterized as *β*-cymarose. Taking *β*-cymaroseII of **1** as an example, in the 1D-TOCSY experiment, irradiation of the signal at δ_H 3.62 (H_{cymII}-3, 1H, dd, *J* = 6.0, 2.9 Hz) enabled identification of H_{cymII}-1 (δ_H 4.67, 1H, dd, *J* = 9.7, 1.6 Hz), H_{cymII}-2a (δ_H 1.62~1.64, 1H, m), H_{cymII}-2b (δ_H 2.23~2.27, 1H, m), H_{cymII}-4 (δ_H 3.19, 1H, dd, *J* =9.7, 2.8 Hz) and H_{cymII}-6 (δ_H 1.27, 1H, d, *J* = 6.2 Hz) in the same conjugation system. According to the coupling constant of each proton signal, the kind of saccharide moiety could be identified. These proton signals were further assigned based on analysis of its ^{1}H-^{1}H COSY spectrum [^{1}H-^{1}H COSY correlations between H_{cymII}-1 (δ_H 4.67) and H_{cymII}-2a (δ_H 1.62~1.64), H_{cymII}-2a (δ_H 1.62~1.64) and H_{cymII}-3 (δ_H 3.62), H_{cymII}-3 (δ_H 3.62) and H_{cymII}-4 (δ_H 3.19), H_{cymII}-4 (δ_H 3.19) and H_{cymII}-5 (δ_H 3.55), H_{cymII}-5 (δ_H 3.55) and H_{cymII}-6 (δ_H 1.27)]. The HMBC spectrum revealed [1]H-^{13}C long-range correlations of H_{cymI}-1 to C-3 (δ_C 74.9); and H_{cymII}-1 to C_{cymI}-4 (δ_C 82.2), which illustrates the connection sequence of oligosaccharide chain and its location at C-3 of the aglycone in compound **1**. In 20-hydroxy-C/D-cis-pregnane-type steroids, steric hindrance between H-16, H-20, H-18 and H-21 of the cyclopentane ring can lead to chemical shifts and is indicative of the absolute configuration of the C-20 [27]. The NOE's between H-9 (δ_H 1.87~1.90) and H-12 (δ_H 4.74~4.77), between H-18 (δ_H 1.60) and H-20 (δ_H 4.84), and our experimental data were similar to the closest structures published in the literature, which led to the deduction of the 20*S* configuration [28–30]. Thus, compound **1** was determined as 12-*O*-cinnamoyl-20-*O*-benzoyl-heptahydroxy-(20*S*)-pregn-6-enyl-3-*O*-*β* cymaropyranoside-(1→4)-*β*-cymaropyranoside.

Compound **2**, was isolated as a white powder. The molecular formula of **2** was determined as $C_{49}H_{70}O_{15}$ by HRESIMS data (*m/z* 921.4578 [M + Na]$^+$, calcd for 921.4607) (Figure S13). The nmR data (Table 1) of **2** were similar to those of **1**, except for the absence of an *O*-benzoyl group and the presence of a 2-methyl-2-butenoyl group [δ_H 6.72–6.77 (1H, m, H-3''), 1.68 (3H, d, *J* = 7.1 Hz, H-4'') and 1.71 (3H, s, H-5''); δ_C 166.1, 128.8, 138.1, 14.5 and 12.2]. The HMBC (Figure S19) correlations from H-20 (δ_H 4.68) to C-1'' (δ_C 166.1) enabled location of the 2-methyl-2-butenoyl group at C-20. The aglycone of **2** was the same as stephanoside K isolated from *Stephanotis lutchuensis* [29]. Finally, the coupling constants of the anomeric proton δ_H 4.81 (1H, dd, *J* = 9.6, 1.8 Hz, H_{cymI}-1) and 4.67 (1H, dd, *J* = 10.0, 2.3 Hz, H_{cymII}-1) illustrated that the sugars were *β*-linkage. By comparison of the ^{1}H and ^{13}C nmR data for **2** with those of **1**, **2** was observed to have the similar aglycone and the same sugar sequence as those of **1**, and the key HMBC correlations confirmed that the sugar moiety was attached to C-3 of the aglycone (Figure 2). Thus, the structure of **2** was elucidated as 12-*O*-cinnamoyl-20-*O*-*(E)*-2-methyl-2-butenoyl-heptahydroxy-(20*S*)-pregn-6-enyl-3-*O*-*β*-cymaropyranoside-(1→4)-*β*-cymaropyranoside.

Table 1. ^{1}H and ^{13}C nmR data of compounds **1** and **2** (δ_H in ppm, *J* in Hz).

No.	1		2	
	δc	δ_H mult. (*J* in Hz)	δc	δ_H mult. (*J* in Hz)
1	26.1	1.53~1.56, m 1.95~1.97, m	26.3	1.50~1.52, m 1.97~1.98, m
2	26.7	1.46~1.50, m 1.77~1.80, m	26.7	1.46~1.50, m 1.77~1.78, m
3	74.9	4.07~4.10, m	74.9	4.07, m
4	38.5	1.6~1.62, m 1.98~2.02, overlap	38.6	1.59~1.60, m 1.99~2.03, m
5	74.6		74.6	
6	136.7	5.63, d, (10)	136.3	5.60, d, (10.3)
7	126.3	5.83, d, (10)	126.4	5.82, d, (10.3)
8	74.3		74.1	
9	36.0	1.87~1.90, overlap	36.0	1.88~1.89, m
10	39.2		39.2	
11	22.7	1.74~1.76, m 1.87~1.90, m	22.8	1.74~1.76, m 1.91~1.92, m
12	74.8	4.74~4.77, m	74.7	4.72, dd, (10.4, 4.4)
13	57.6		57.4	
14	87.8		88.0	
15	32.1	1.70~1.73, m 1.91~1.94, m	32.3	1.72~1.73, m 1.89~1.91, m
16	33.5	1.98~2.02, overlap	33.1	1.93~1.95, overlap
17	87.5		87.4	
18	11.5	1.60, s	11.5	1.53, s
19	21.1	1.01, s	21.1	1.03, s
20	74.7	4.84, q, (6.1)	73.9	4.67~4.69, m
21	15.4	1.35, d, (6.2)	15.3	1.22, d, (6.2)
1′	166.6		166.5	
2′	118.9	6.07, d, (16)	119.1	6.22, d, (16)
3′	144.3	7.42, d, (16)	144.2	7.53, d, (16)
4′	134.4		134.6	
5′(9′)	128.3	7.24, d, (7.3)	128.2	7.45~7.47, m
6′(8′)	128.5	7.30~7.36, overlap	128.9	7.36~7.38, overlap
7′	130.2	7.30~7.36, overlap	130.3	7.36~7.38, overlap
1″	165.0		166.1	
2″	130.4		128.8	
3″	129.9	7.92, d, (7.2)	138.1	6.72~6.77, m
4″	128.7	7.30~7.36, overlap	14.5	1.68, d, (7.1)
5″	133.1	7.53, t, (7.4)	12.2	1.71, s
		cymI		cymI
1	97.7	4.81, dd, (9.7, 1.6)	97.7	4.81, dd, (9.6, 1.8)
2	35.5	1.57~1.59, m 2.11~2.14, m	35.5	1.58~1.59, m 2.11~2.14, m
3	77.1	3.79~3.81, m	77.1	3.80, dd, (5.8, 3.0)
4	82.2	3.24, dd, (9.7, 2.8)	82.2	3.24, dd, (9.7, 2.9)
5	68.8	3.85, dq, (9.6, 6.1)	68.8	3.85, dq, (9.6, 6.2)
6	18.2	1.21, d, (6.2)	18.2	1.20, d, (6.2)
OMe	58.2	3.45, s	58.2	3.44, s
		cymII		cymII
1	99.5	4.67, dd, (9.7, 1.6)	99.5	4.66, dd, (10.0, 2.3)
2	33.8	1.62~1.64, m 2.23~2.27, m	33.8	1.62~1.63, m 2.24~2.26, m
3	77.5	3.62, dd, (6.0, 2.9)	77.5	3.62, dd, (6.2, 3.1)
4	72.5	3.19, dd, (9.7, 2.8)	72.5	3.17~3.21, m
5	70.9	3.55, dq, (9.6, 6.1)	70.9	3.55, dq, (9.6, 6.2)
6	18.5	1.27, d, (6.2)	18.5	1.27, d, (6.2)
OMe	57.4	3.42, s	57.4	3.42, s

^{1}H nmR and ^{13}C nmR were measured at 600 and 150 MHz in CDCl$_3$.

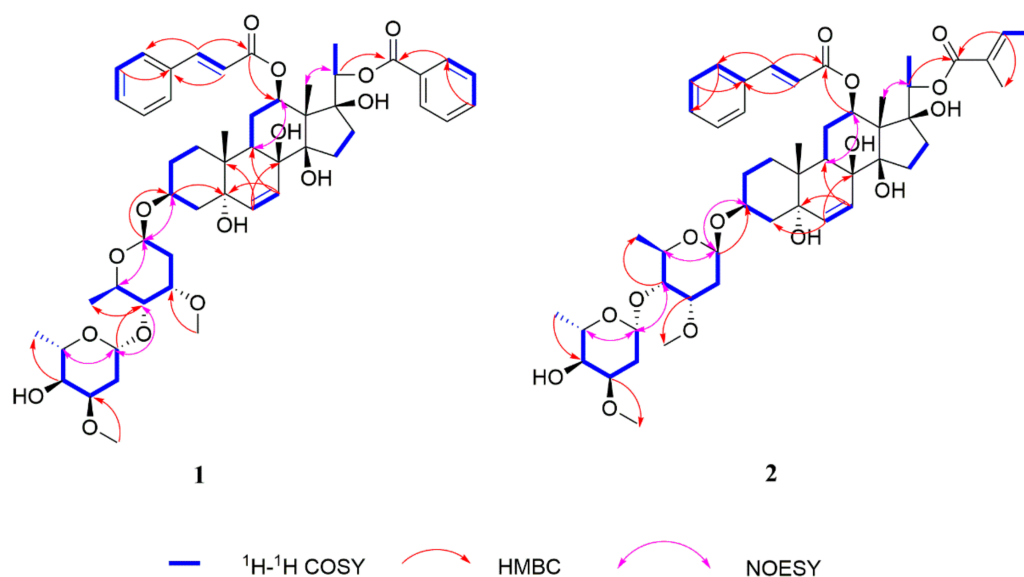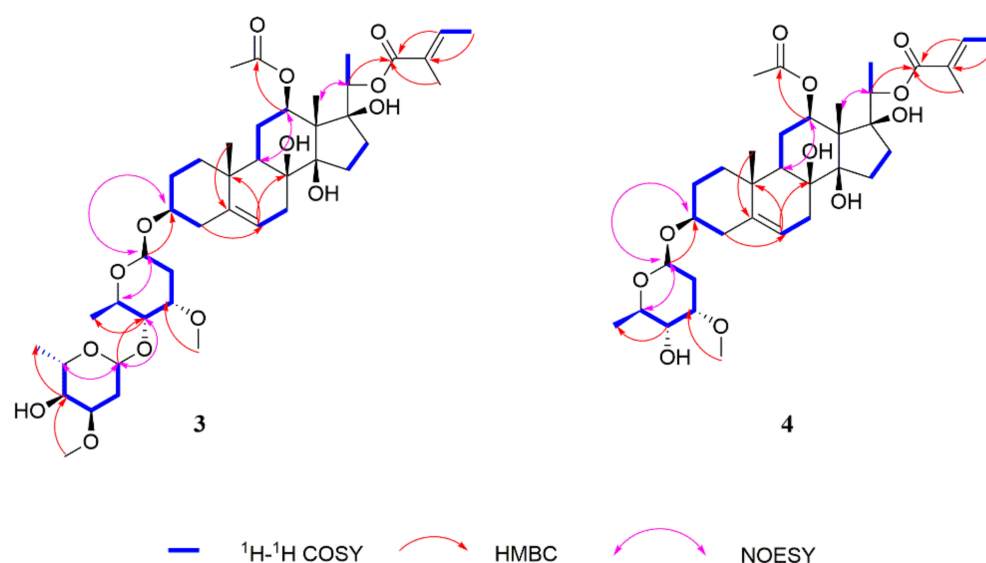**Figure 2.** Key ^{1}H-^{1}H COSY and HMBC correlations of **1** and **2**.

Compound **3** was isolated as a white powder. The molecular formula was established as $C_{42}H_{66}O_{14}$ by HRESIMS data (*m/z* 817.4339, [M + Na]$^{+}$, calcd for 817.4350) (Figure S25). The IR spectrum of **3** (Figure S36) showed the characteristic for hydroxy (3441 cm^{-1}), ester (1701 cm^{-1}) and olefinic (1681 cm^{-1}) groups. By comparison of the nmR (Table 2) data of **3** with **1**, compound **3** show the similar skeleton with **1**, but the presence of the key HMBC (Figure S31) long-range correlations of δ_H 2.36~2.40 (H-4) to δ_C 118.4 (C-6), δ_H 5.36~5.38 (H-6) to δ_C 74.2 (C-8) and 37.1 (C-10), and δ_H 1.13 (H-19) to δ_C 139.9 (C-5) explained that the double bond was located at H-5 and H-6. In addition, the ^{13}C nmR spectroscopic data of the skeleton of **3** matched well with those of the sarcostin skeleton isolated from *Cynanchum* botanicals [31,32]. By detailed analyses of its HSQC, ^{1}H-^{1}H COSY and HMBC spectra (Figures S29–S31), a 2-methyl-2-butenoyl group [δ_H 6.83~6.87 (1H, m, H-3′), 1.82 (3H, d, *J* = 7.0 Hz, H-4′) and 1.85 (3H, s, H-5′); δ_C 166.4 (C-1′), 128.8 (C-2′), 138.0 (C-3′), 14.7 (C-4′) and 12.3 (C-5′)] and an acetyl group [δ_H 1.94 (3H, s, H-2″); δ_C 171.3 (C-1″) and 21.9 (C-2″)] were also observed. The key HMBC correlations of δ_H 4.65~4.66 (1H, m, H-20) to δ_C 166.4 (C-1′), and δ_H 4.62 (1H, dd, *J* = 11.3, 4.0 Hz, H-12) to δ_C 171.3 (C-1″) revealed the placement of the two ester groups at C-20 and C-12, respectively. The aglycone of **3** was the same as marstomentoside J isolated from *Marsdenia tomentosa* [33]. The ^{1}H nmR spectrum of **3** showed two anomeric proton signals at δ_H 4.84 (1H, dd, *J* = 9.6, 1.7 Hz, H$_{cymI}$-1) and 4.67 (1H, dd, *J* = 9.5, 1.8 Hz, H$_{cymII}$-1), and the coupling constants of the anomeric protons illustrated that the sugars were *β*-linkage. By comparison of the ^{1}H and ^{13}C nmR data for **3** with those of **1**, **3** was observed to have the similar aglycone and the same sugar sequence as those of **1**, and the key HMBC correlations confirmed that the sugar moiety was also attached to C-3 of the aglycone (Figure 3). Based on the above evidence, the absolute configuration of **3** was elucidated as 12-*O*-acetyl-20-*O*-(*E*)-2-methyl-2-butenoyl-sarcostin-(20S)-3-*O*-β-cymaropyranoside-(1→4)-β-cymaropyranoside.

Table 2. [1]H and[13] C nmR data of compounds **3** and **4** (δ_H in ppm, *J* in Hz).

No.	3		4	
	δc	δ_H mult. (*J* in Hz)	δc	δ_H mult. (*J* in Hz)
1	38.9	1.06~1.10, m 1.83~1.84, overlap	38.9	1.08, dd, (13.5, 3.5) 1.83~1.84, overlap
2	29.1	1.63~1.64, m 1.89~1.93, overlap	29.1	1.61~1.64, m 1.87~1.92, overlap
3	78.1	3.54~3.56, m	77.9	3.53~3.56, m
4	38.9	2.29~2.32, m 2.36~2.40, m	38.8	2.29~2.32, m 2.36~2.39, m
5	139.9		139.7	
6	118.4	5.36~5.38, m	118.6	5.36~5.37, m
7	34.6	2.14~2.17, m	34.6	2.14~2.17, m
8	74.2		74.2	
9	43.4	1.45~1.47, overlap	43.4	1.44~1.46, overlap
10	37.1		37.1	
11	24.9	1.65~1.67, m 1.89~1.93, overlap	24.9	1.64~1.66, m 1.87~1.92, overlap
12	73.6	4.62, dd, (11.3, 4.0)	73.6	4.62, dd, (11.5, 4.2)
13	56.2		56.2	
14	88.0		87.9	
15	32.0	1.87~1.89, overlap 1.89~1.93, overlap	31.8	1.86~1.88, overlap 1.90~1.93, overlap
16	33.2	1.87~1.89, overlap 1.89~1.93, overlap	33.2	1.86~1.88, overlap 1.90~1.93, overlap
17	87.9		88.1	
18	10.4	1.44, s	10.4	1.44, s
19	18.3	1.13, s	18.3	1.14, s
20	74.2	4.65~4.66, m	74.2	4.65, q, (6.2)
21	15.1	1.23, d, (5.6)	15.1	1.22, d, (6.1)
1′	166.4		166.4	
2′	128.8		128.8	
3′	138.0	6.83~6.87, m	138.1	6.83~6.87, m
4′	14.7	1.82, d, (7.0)	14.8	1.81, d, (7.1)
5′	12.3	1.85, s	12.3	1.85, s
1″	171.3		171.3	
2″	21.9	1.94, s	21.9	1.94, s
		cymI		cym
1	96.2	4.84, dd, (9.7, 1.7)	95.7	4.78, dd, (9.6, 1.8)
2	35.6	1.55~1.59, m 2.09~2.12, m	34.2	1.57~1.60, m 2.19~2.22, m
3	77.2	3.81, dd, (5.9, 2.8)	77.6	3.62, dd, (6.1, 3.0)
4	82.6	3.22, dd, (9.7, 2.9)	72.6	3.21, dd, (9.5, 3.6)
5	68.6	3.85, dq, (9.6, 6.1)	70.9	3.57, dq, (9.7, 6.1)
6	18.3	1.22, d, (6.0)	18.4	1.27, d, (6.2)
OMe	58.1	3.44, s	57.4	3.43, s
		cymII		
1	99.5	4.67, dd, (9.5, 1.8)		
2	33.8	1.60~1.62, m 2.23~2.26, m		
3	77.5	3.62, (6.2, 3.1)		
4	72.5	3.19, dd, (9.7, 3.6)		
5	70.8	3.55, dq, (9.5, 6.2)		
6	18.5	1.27, d, (6.2)		
OMe	57.4	3.42, s		

[1]H nmR and ^{13}C nmR were measured at 600 and 150 MHz in CDCl$_3$.

Figure 3. Key ^{1}H–^{1}H COSY and HMBC correlations of **3** and **4**.

Compound **4** was isolated as a white powder. The molecular formula was established as $C_{35}H_{54}O_{11}$ by HRESIMS data *m/z* 673.3553 [M + Na]$^+$, (calcd for 673.3564) (Figure S37). The nmR data (Table 2) of **4** were very similar to those of **3**, except for the absence of one sugar group [δ_C 99.5, 33.8, 77.2, 82.6, 68.6, 18.3, 58.1]. The ^{1}H nmR spectrum of **4** showed one anomeric proton signal at δ_H 4.78 (1H, dd, *J* = 9.6, 1.8 Hz), and the coupling constants of the anomeric proton illustrated that the sugar was *β*-linkage. In addition, the key HMBC (Figure S43) correlations confirmed that the sugar moiety was also attached to C-3 of the aglycone. Thus, the structure of **4** was characterized as 12-*O*-acetyl-20-*O*-(*E*)-2-methyl-2-butenoyl-sarcostin-(20*S*)-3-*O*-*β*-cymaropyranoside.

Four known compounds were also isolated and identified as gymnepregoside H (**5**), [23] deacetylkidjoladinin (**6**), [34] gymnepregoside G (**7**) [23] and gymnepregoside I (**8**) [35], by comparison of spectroscopic data and physicochemical properties with those reported values in the literatures.

Researches showed that berberine has been shown to have antidiabetic properties. Berberine could downregulated the expression of genes involved in lipogenesis and up-regulated those involved in energy expenditure in adipose tissue and muscle [36,37]. The abundant compounds **1**–**6** (>2 mg) were selected to evaluate their glucose uptake activity in L6 cells. Berberine (BBR, 30 μg/mL) was used as the positive control, and we used a cell-based fluorescently-labeled deoxyglucose analog kit to test the uptake activity. After incubating with samples, the 2-NBDG fluorescence intensity at the plasma membrane shows varying degrees of change. Compared to normal control (NC) group, three new compounds sylvepregosides B-D (**2**–**4**) and deacetylkidjoladinin (**6**) exerted weak activity, and showed glucose uptake activity with the enhancement by 0.2-, 0.16-, 0.13- and 0.1-fold at 30 μg/mL (Figure 4). Gymnepregoside H (**5**) possesses a moderate effect on promoting glucose uptake, which increased glucose uptake to 1.96 folds at 30 μg/mL. Sylvepregosides A (**1**) was the most active compound, and exhibited glucose uptake activity with 1.37-fold enhancement at 30 μg/mL. Comparing **1** and **5**, both exhibited two groups of aromatic signals on C-12 and C-20, the only difference was the oligosaccharide chain in compound **1**, whereby the polysaccharide may enhance the activities of glucose uptake.

For further evaluation of the efficacy of **1** and **5**, a L6 cell line which stably expressed Myc-GLUT4-mOrange was used to test whether samples could also facilitate the fusion of GLUT4 with the plasma membrane. The red fluorescence of GLUT4-mOrange and the green fluorescence of FITC-myc were detected using laser confocal microscopy. As a result, we found that gymnepregoside H (**5**) possesses a moderate effect on promoting GLUT-4 fusion with the plasma membrane in L6 cells. Sylvepregosides A (**1**) was the most active

compound promoting GLUT-4 fusion with the plasma membrane in L6 cells (Figure 5). Quantification of this effect revealed that the percentage of FITC positive cells were 69% and 65%, respectively (Figure 6).
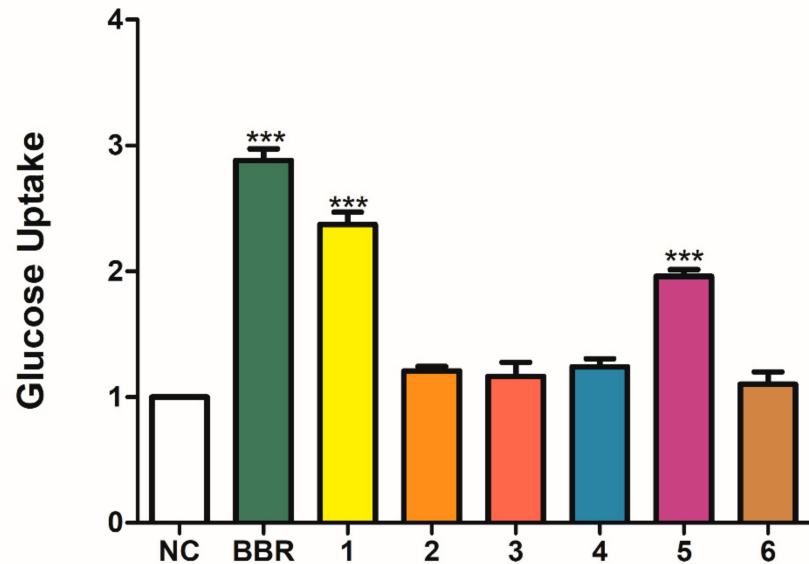

Figure 4. Effects of compounds **1–6** (30 μg/mL) on glucose uptake in L6 cells. Glucose uptake activities of compounds **1–6** in L6 cells using a fluorescent derivative of glucose, 2-NBDG. Berberine (30 μg/mL) was used as a positive control. After incubation for 24 h with or without 2-NBDG, the fluorescent signals were detected at Ex/Em = 485/535 nm. The results were calculated as the means $\pm$ standard error of mean (n = 5), with each performed five times; * $p < 0.05$, ** $p < 0.01$, and *** $p < 0.001$, compared to non-control group.
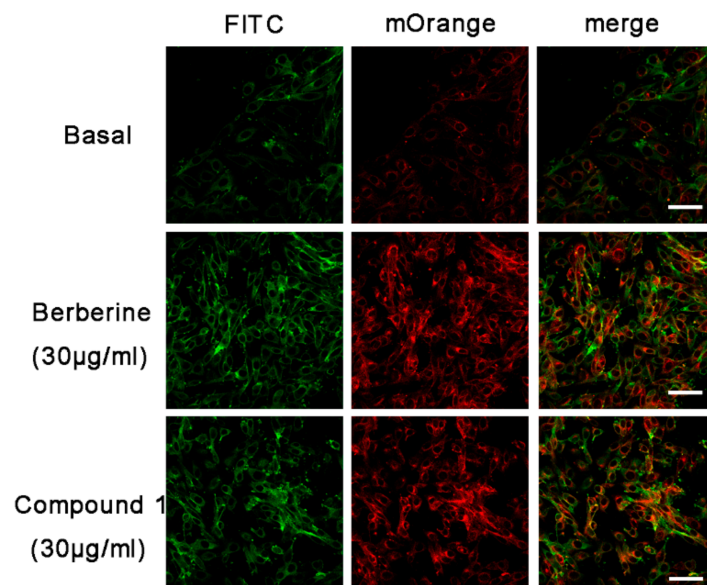
Figure 5. Effect of compounds **1** on fusion of GLUT4 with the plasma membrane in L6 cells. Berberine (30 μg/mL) was used as a positive control. FITC fluorescence assay in myc-GLUT4-mOrange cells treated with 30 μg/mL of compound **1** or berberine. Scale bar = 50 μm.
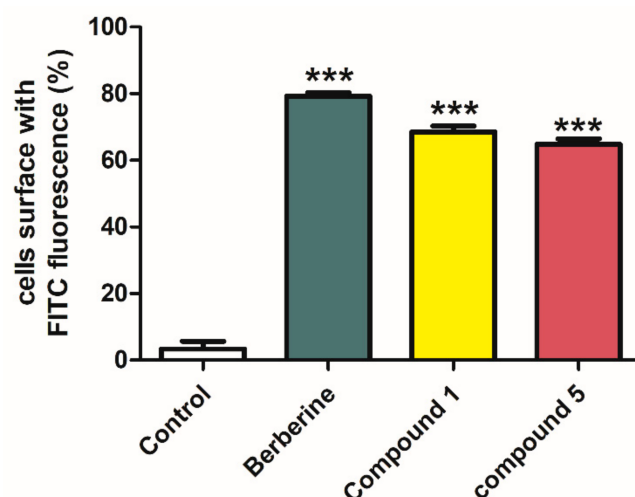
Figure 6. Quantitation of FITC green fluorescence cells. Treatment with 30 μg/mL of berberine or 30 μg/mL of compounds **1** and **5** for 30 min significantly increases fusion of GLUT4 with the plasma membrane in L6 cells. The results were calculated as the means ± standard error of mean (n = 3), with each performed three times; * $p < 0.05$, ** $p < 0.01$, and *** $p < 0.001$, compared to control group.

3. Materials and Methods

3.1. Chemicals and Reagents

Chromatography grade solvents were used for HPLC, and all other chemical reagents were analytical grade. HPLC grade acetonitrile and methanol were purchased from Merck (Darmstadt, Germany). Sephadex LH-20 dextran gel was purchased from Amersham Pharmacia Biotech Co. (Piscataway, NJ, USA).

3.2. General Experimental Procedures

Semi-preparative HPLC purification was performed on a Waters 2535 HPLC connected with a 2998 PDA Detector and a 2707 Autosampler (Waters, Milford, MA, USA). Separations were performed on a COSMOSIL C18 column (5 μm, 10 × 250 mm) (Nacalai Tesque, Kyoto, Japan), a COSMOSIL C8 column (5 μm, 10 × 250 mm) (Nacalai Tesque, Kyoto, Japan) and a YMC-pack diol column (5 μm, 10 × 50 mm; 5 μm, 20 × 150 mm) (Yamamura Chemical Research, Kyoto, Japan). Direct injection high resolution ESIMS and LC-DAD-ESIMS analyses were recorded on an ultra-performance liquid chromatography-quadrupole/electrostatic field orbitrap high resolution mass spectrometry (Thermo Fisher Scientific, Waltham, MA, USA). The nmR spectra were recorded on an AVANCE III 600 MHz spectrometer (Bruker BioSpin, Ettlingen, Germany). Optical rotations were recorded on an Autopol IV Automatic Polarimeter (Rudolph Research Analytical, Hackettstown, NJ, USA).

3.3. Materials

The aerial part of *G. sylvestre* were collected from Nanning, Guangxi, China, in June 2019. The roots were dried at room temperature, macerated into a fine powder, and stored at room temperature. The plant was identified by Professor Songji Wei of School of Pharmaceutical Sciences, Guangxi University of Chinese medicine, Nanning, China.

3.4. Extraction and Isolation

The dried aerial parts of the plant (15.0 kg) were milled and then extracted with 70% EtOH (3 × 20 L, 3 days each) at room temperature to yield 1752.1 g of crude extract. Subsequently, the crude extract was suspended in H_2O and partitioned with petroleum ether (PE) (8 × 10 L), ethyl acetate (EtOAc) (8 × 10 L), and n-butyl alcohol (n-BuOH) (8 × 10 L) to give a PE fraction (73.1 g), EtOAc fraction (383.3 g), and n-BuOH fraction (758.0 g), respectively. The EtOAc fraction (360.0 g) was subjected to HP-20 column (6 × 61 cm) chromatography eluting with a gradient solvent system of EtOH /H_2O (10%,

30%, 50%, 70%, 80%, 95%), to yield six major fractions FA1–FA6. FA6 (75.0 g) was separated on a silica-gel column chromatography (300–400 mesh), using CH_2Cl_2/MeOH (100:1, 80:1, 50:1, 30:1, 20:1, 9:1, 7:1, 5:1, 3:1, 1:100, *v/v*) as a mobile phase, to obtain ten fractions FA6-1-FA6-10. FA6-5 (2.2 g) was further separated by the Sephadex LH-20 and eluted with MeOH to give six subfractions FA6-5-1–FA6-5-6. FA6-5-2 (1.9 g) by using semi-preparative HPLC (MeCN /H_2O, 50:50–100:0, 25 min) at a rate of 4 mL/min, an injection volume of 200 μL and UV at 200 nm with column temperature at 30 °C to obtain four fractions FA6-5-2-1–FA6-5-2-4. FA6-5-2-4, by using semi-preparative HPLC [n-Hexane/n-Hexane: iso-Propyl alcohol (7:3), 40:60–0:100, 30 min] at a rate of 4 mL/min, an injection volume of 150 μL and UV at 200 nm with column temperature at 30 °C to obtain compound **1** (t_R = 23.10 min; 5.3 mg) and compound **2** (t_R = 22.04 min; 5.0 mg). Purification of fraction FA6-5-2-3 with n-Hexane/n-Hexane: iso-Propyl alcohol (7:3), 22:78, 30 min at a rate of 9 mL/min, an injection volume of 300 μL and UV at 200 nm, with column temperature at 30 °C, to afford **3** (t_R = 26.87 min; 5.1 mg) and **5** (t_R = 35.98 min; 8.9 mg) by using the YMC-pack Diol column. FA6-5-2-2, using the YMC-pack Diol column with [n-Hexane/n-Hexane: iso-Propyl alcohol (7:3), 75:25–55:45, 30 min] at a rate of 4 mL/min, an injection volume of 100 μL and UV at 200 nm, with column temperature at 30 °C, to give compound **4** (t_R = 15.06 min; 4.5 mg) and compound **8** (t_R = 16.38 min; 1.7 mg). FA6-5-2-1, by using the YMC-pack Diol column with [n-Hexane/n-Hexane: iso-Propyl alcohol (7:3), 90:1–0:100, 20 min] at a rate of 4 mL/min, an injection volume of 100 μL and UV at 200 nm, with column temperature at 30 °C, to give compound **6** (t_R = 16.80 min; 5.5 mg) and compound **7** (t_R = 15.46 min; 1.4 mg).

3.4.1. Sylvepregosides A (**1**)

White powder; $[\alpha]^{20}_D$ +147.3 (*c* 0.50, MeOH); UV (MeOH, nm) λ_{max} (log ε) = 230.0 (3.35), 280 (3.32) nm; IRν_{max} = 3480, 2930, 1713, 1689, 1281, 1169, 1065 and 1005 cm^{-1}; For ^{1}H nmR (600 MHz) and ^{13}C nmR (150 MHz) data can be found in Table 1; HRESIMS *m/z* 943.4423 [M + Na]$^+$ (calcd for $C_{51}H_{68}O_{15}$ Na: 943.4450)

3.4.2. Sylvepregosides B (**2**)

White powder; $[\alpha]^{20}_D$ + 145.8 (c 0.50, MeOH); UV (MeOH, nm) λ_{max} (log ε) = 210 (1.60), 280 (1.36) nm; IRν_{max} = 3482, 2920, 1707, 1685, 1273, 1169, 1067, 1005 and 981 cm^{-1}; For ^{1}H nmR (600 MHz) and ^{13}C nmR (150 MHz) data can be found in Table 1; HRESIMS *m/z* 921.4578 [M + Na]$^+$ (calcd for $C_{26}H_{31}O_7$ Na: 921.4607).

3.4.3. Sylvepregosides C (**3**)

White powder; $[\alpha]^{20}_D$ +56.9 (c 0.50, MeOH); UV (MeOH, nm) λ_{max} (log ε) = 215 (0.50); IRν_{max} = 3441, 2940, 1701, 1681, 1236, 1082 and 983 cm^{-1}; For ^{1}H nmR (600 MHz) and ^{13}C nmR (150 MHz) data can be found in Table 2; HRESIMS m/z 817.4339 [M + Na]$^+$ (calcd for $C_{42}H_{66}O_{14}$Na: 817.4350).

3.4.4. Sylvepregosides D (**4**)

White powder; $[\alpha]^{20}_D$ +32 (*c* 0.50, MeOH); UV (MeOH, nm) λ_{max} (log ε) = 210 (1.19); IR ν_{max} = 3402, 2933, 1705, 1676, 1269, 1080 and 983 cm^{-1}; For ^{1}H nmR (600 MHz) and ^{13}C nmR (150 MHz) data can be found in Table 2; HRESIMS *m/z* 673.3553 [M + Na]$^+$ (calcd for $C_{35}H_{54}O_{11}$ Na: 673.3564).

3.5. Glucose Uptake and GLUT-4 Fusion with the Plasma Membrane

3.5.1. Propagation and Maintenance of L6 Cells

For the L6 cells (Rat skeletal muscle), cell culture was procured from the American Type Culture Collection (ATCC), Manassas, Commonwealth of Virginia, America. L6 cells were cultured and maintained in α- minimum essential medium (α-MEM) with 2% inactivated fetal bovine serum (FBS) along with penicillin (100 μg/mL) and streptomycin (100 μg/mL), in a humidified atmosphere of 5% CO_2 at 37 °C until confluent. The medium

was changed every 24 h and cultured for 7 days to promote the differentiation of L6 cells into myotube cells. α-MEM, FBS, penicillin and streptomycin were obtained from Hyclone (Logan, UT, USA). The stock cultures were grown in 25 cm² culture flasks, and the experiments were carried out in 60 mm petri dishes and 96-well microtiter plates. We used R-250 (Coomassie blue) staining to identify the difference between myotubes and normal L6 cells, the difference was the myotubes showed increasing cytoplasmic tonofilaments [38].

3.5.2. Glucose Uptake Assay

Differentiated L6 myotubes were seeded in a 96-well black plate with the density of 1×10^4–5×10^4 cells/well and incubated in 100 μL α-MEM for 12 h until 100% confluence. Thereafter, L6 cells were treated with proper dosages of sample or berberine dispersed in 100 μL glucose-free α-MEM dissolved in 150 μg/mL 2-NBDG (Cayman Chemical, Ann Arbor, MI, USA). After 24 h incubation in the cell incubator, the 96-well black plate was centrifuged for 5 min at $400\times g$ at room temperature. Discarding the supernatant, 200 μL cell-based assay buffer was added into each well, and then the 96-well black plate was centrifuged for 5 min at $400\times g$ at room temperature. After aspirating the cell-based assay buffer, each well was added into 100 μL of assay buffer. Finally, we set the excitation/emission of the fluorescent microplate reader at 485/535 nm and analyzed fluorescence intensity of 2-NBDG in each well. Zen 2010 Software (Carl Zeiss, Jena, Germany) was used to analyze the fluorescence intensity of 2-NBDG.

3.5.3. GLUT-4 Fusion with the Plasma Membrane

Construction of the myc-GLUT4-mOrange plasmid and cell line was performed as described previously [39] GLUT-4 fusion with the plasma membrane Myc-GLUT4-mOrange cells were cultured in six-well plates and grown on coverslips. After 2 h of starvation treatment, the cells were incubated in the presence of sample or berberine for 30 min. Then, cells were fixed with 3% polyformaldehyde for 30 min. After blocking with 2% bovine serum albumin (BSA; Hyclone, Logan, UT, USA) in phosphate buffered saline (PBS; Hyclone, Logan, UT, USA) for 30 min at room temperature, the cells were incubated with anti-myc mouse monoclonal antibody (TransGen Biotech, Beijing, China) for 1 h at room temperature. Then, the cells were washed three times with 2% BSA in PBS and incubated with goat anti-mouse-FITC (TransGen Biotech, Beijing, China). After being washed three times with 2% BSA in PBS, the coverslips were turned over and placed on a glass slide. Finally, mOrange red fluorescence and FITC green fluorescence were observed using a laser confocal microscope. GLUT-4 externalization was quantitated by determination of the percentage of GLUT4-mOrange-positive cells that exhibited FITC fluorescence at the cell surface.

3.6. Statistical Analysis

Differences between groups were analyzed by one-way analysis of variance (ANOVA). Data are shown as means ± standard error (M ± SEM). Tukey's post hoc test of Graph-Pad Prism 5.0 software packages was used to perform statistical analyses. A probability (*p*) values < 0.05 were regarded as statistically significant.

4. Conclusions

In this study, four new C_{21} steroidal glycosides sylvepregosides A-D (**1–4**), as well as four known compounds (**5–8**) were obtained from *Gymnema sylvestre*. Compounds **1–6** presented the effects of glucose uptake in L6 cells at 1.10- to 2.37-fold, respectively. Specifically, compound **1** exerted the strongest activity for glucose uptake, with 1.37-fold enhancement, and compound **5** showed moderate uptake activity, by increasing glucose uptake by 0.96-fold. Further study shows that compounds **1** and **5** could promote GLUT4 fusion with the plasma membrane in L6 cells. Our research suggested that compounds **1** and **5** could offer promising lead structures with glucose uptake activity, which could be

meaningful to the development of pharmaceutical products. Meanwhile, it also provided a clue for potentially active anti-diabetic constituents in the plants of genus *Gymnema*.

References

1. Li, K.D.; Ma, Y.R.; Zhou, T.X.; Yang, X.Z.; Choi, H.Y. Chemical constituents from roots of *Sophora davidii* (Franch.) Skeels and their glucose transporter 4 translocation activities. *Molecules* **2021**, *26*, 756. [CrossRef] [PubMed]
2. Li, Y.J.; Tang, Y.L.; Shi, S.R.; Gao, S.J.; Wang, Y.; Xiao, D.X.; Chen, T.Y.; He, Q.; Zhang, J.J.; Lin, Y.F. Tetrahedral framework nucleic acids ameliorate insulin resistance in type 2 diabetes mellitus via the PI3K/Akt pathway. *ACS Appl. Mater. Interfaces* **2021**, *13*, 40354–40364. [CrossRef]
3. Keane, K.N.; Cruzat, V.F.; Carlessi, R.; de Bittencourt, P.I.J.; Newsholme, P. Molecular events linking oxidative stress and inflammation to insulin resistance and β-cell dysfunction. *Oxid. Med. Cell. Longev.* **2015**, *2015*. [CrossRef]
4. Xu, L.; Li, Y.; Dai, Y.; Peng, J. Natural products for the treatment of type 2 diabetes mellitus: Pharmacology and mechanisms. *Pharm. Res.* **2018**, *130*, 451–465. [CrossRef]
5. Editorial Committee of Chinese of Flora China Academy of Sciences. *Flora China*; Science Press: Beijing, China, 1977; p. 418.
6. National Chinese Herbal Medicine Compilation Compilation Group. *The Compilation of National Chinese Herbal Medicine*; People's Medical Publishing House: Beijing, China, 1978; p. 573.
7. Xiang, J.M.; Wei, J.H.; Xiao, W.; Xu, J.L.; Xiao, P.G. Research progress in *Gymnema sylvestre* (Retz.) Schult. *Res. Pract. Chin. Med.* **2018**, *32*, 77–78. [CrossRef]
8. Tiwari, P.; Mishra, B.N.; Sangwan, N.S. Phytochemical and pharmacological properties of *Gymnema sylvestre*: An important medicinal plant. *Biomed. Res. Int.* **2014**, *2014*, 830285. [CrossRef]
9. Zhu, H. National medicine clinical progress of the treatment of diabetic. *J. Med. Pharm. Chin. minorities* **2008**, *6*, 68–70. [CrossRef]
10. Kang, M.H.; Lee, M.S.; Choi, M.K.; min, K.S.; Shibamoto, T. Hypoglycemic activity of *Gymnema sylvestre* extracts on oxidative stress and antioxidant status in diabetic rats. *J. Agric. Food Chem.* **2012**, *60*, 2517–2524. [CrossRef] [PubMed]
11. Huang, K.S.; Wang, Y.H.; Li, R.L.; Lin, M. Study on the hypoglycemic pharmacological action of the root of *Gymnema sylvestre* (Retz) Schult. *Phytochemistry* **2000**, *54*, 875–881. [CrossRef]
12. Ramar, K.; David Adedayo Animasaun, R.T. Patel, Rajashekhar Ingalhalli. Phytochemical constituents and hypoglycemic effect of gymnemin acid extracts from big and small leaf varieties of *Gymnema sylvestre* R. Br. *Indonesian J. Pharm.* **2016**, *27*, 59–65. [CrossRef]
13. Zhu, X.M.; Xie, P.; Di, Y.T.; Peng, S.L.; Ding, L.S.; Wang, M.K. Two new triterpenoid saponins from *Gymnema sylvestre*. *J. Integr. Plant Biol.* **2008**, *50*, 589–592. [CrossRef]
14. Arumugam, R.; Govindarajan, S. Histological studies on pancreatic tissue in high fat diet with low multiple dosage of streptozotocin induced type 2 diabetes after *Gymnema sylvestre* administration. *Indian J. Public Health* **2019**, *10*, 917–922. [CrossRef]
15. Gaytán Martínez, L.A.; Sánchez-Ruiz, L.A.; Zuñiga, L.Y.; González-Ortiz, M.; Martínez-Abundis, E. Effect of *Gymnema sylvestre* administration on glycemic control, insulin secretion, and insulin sensitivity in patients with impaired glucose tolerance. *J. Med. Food* **2021**, *24*, 28–32. [CrossRef]

16. Ulbricht, C.; Abrams, T.R.; Basch, E.; Davies-Heerema, T.; Foppa, I.; Hammerness, P.; Rusie, E.; Tanguay-Colucci, S.; Taylor, S.; Ulbricht, C.; et al. An evidence-based systematic review of gymnema (*Gymnema sylvestre* R. Br.) by the natural standard research collaboration. *J. Diet. Suppl.* **2011**, *8*, 311–330. [CrossRef]

17. Kumar, P.M.; Venkataranganna, M.V.; Manjunath, K.; Viswanatha, G.L.; Ashok, G. Methanolic leaf extract of *Gymnema sylvestre* augments glucose uptake and ameliorates insulin resistance by upregulating glucose transporter-4, peroxisome proliferator-activated receptor-gamma, adiponectin, and leptin levels in vitro. *J. Intercult. Ethnopharmacol.* **2016**, *5*, 146–152. [CrossRef]

18. Patel, K.; Gadewar, M.; Tripathi, R. Pharmacological and analytical aspects of gymnemic acid: A concise report. *Asian Pac. J. Trop. Dis.* **2012**, *2*, 414–416. [CrossRef]

19. Li, Y.M.; Liu, Y.P.; Liang, J.J.; Wang, T.X.; Sun, M.Z.; Zhang, Z.S. Gymnemic acid ameliorates hyperglycemia through PI3K/AKT- and AMPK-Mediated signaling pathways in type 2 diabetes mellitus rats. *J. Agric. Food Chem.* **2019**, *67*, 13051–13060. [CrossRef]

20. Wang, Y.; Dawid, C.; Kottra, G.; Daniel, H.; Hofmann, T. Gymnemic acids inhibit sodium-dependent glucose transporter 1. *J Agric. Food Chem.* **2014**, *62*, 5925–5931. [CrossRef] [PubMed]

21. Lin, L.; Chen, Y.W.; Wang, L.Y.; Tang, X.Q. Research progress on pharmacological action of *Gymnema sylvestre* (Retz.) Schult. *Chin. Tradit. Pat. Med.* **2013**, *35*, 1748–1751. [CrossRef]

22. Qiu, Q.; Zhen, H.S.; Wei, Y.F.; Zhen, D.D. Research Progress on Effective substance and quality analysis of *Gymnema sylvestre* (Retz.) schult. *Chin. J. Ethnomed. Ethnopharm.* **2017**, *26*, 51–53.

23. Lin, Y.L.; Wu, Y.M.; Kuo, Y.H.; Chen, C.F. Pregnane glycosides from *Gymnema alternifolium*. *J. Chin. Chem. Soc.* **2013**, *46*, 841–846. [CrossRef]

24. Yoshikawa, K.; Matsuchika, K.; Arihara, S.; Chang, H.C.; Wang, J.D. Pregnane glycosides, gymnepregosides A-F from the roots of *Gymnema alternifolium*. *Chem. Pharm. Bull.* **1998**, *46*, 1239–1243. [CrossRef]

25. Li, X.; Sun, H.; Ye, Y.; Chen, F.; Tu, J.; Pan, Y. Four new immunomodulating steroidal glycosides from the stems of *Stephanotis mucronata*. *Steroids* **2006**, *71*, 683–690. [CrossRef]

26. Li, J.L.; Zhou, J.; Chen, Z.H.; Guo, S.Y.; Li, C.Q.; Zhao, W.M. Bioactive C_{21} steroidal glycosides from the roots of *Cynanchum otophyllum* that suppress the seizure-like locomotor activity of zebrafish caused by pentylenetetrazole. *J. Nat. Prod.* **2015**, *78*, 1548–1555. [CrossRef]

27. Tsoukalas, M.; Muller, C.D.; Lobstein, A.; Urbain, A. Pregnane glycosides from *Cynanchum marnierianum* stimulate GLP-1 secretion in STC-1 cells. *Planta Med.* **2016**, *82*, 992–999. [CrossRef] [PubMed]

28. Xu, R.; Yang, Y.; Zhang, Y.; Ren, F.; Xu, J.; Yu, N.; Zhao, Y. New pregnane glycosides from *Gymnema sylvestre*. *Molecules* **2015**, *20*, 3050–3066. [CrossRef]

29. Yoshikawa, K.; Okada, N.; Kan, Y.; Arihara, S. Steroidal glycosides from the fresh stem of *Stephanotis lutchuensis* var. japonica (Asclepiadaceae). Chemical structures of stephanosides K-Q. *Chem. Pharm. Bull.* **1996**, *44*, 2243–2248. [CrossRef] [PubMed]

30. Trang, D.T.; Yen, D.T.H.; Cuong, N.T.; Anh, L.T.; Hoai, N.T.; Tai, B.H.; Doan, V.V.; Yen, P.H.; Quang, T.H.; Nhiem, N.X.; et al. Pregnane glycosides from *Gymnema inodorum* and their α-glucosidase inhibitory activity. *Nat. Prod. Res.* **2021**, *35*, 2157–2163. [CrossRef]

31. Li, J.L.; Gao, Z.B.; Zhao, W.M. Identification and evaluation of antiepileptic activity of C_{21} steroidal glycosides from the roots of *Cynanchum wilfordii*. *J. Nat. Prod.* **2016**, *79*, 89–97. [CrossRef]

32. Shi, L.M.; Liu, W.H.; Yu, Q.; Wan, H.T. Two New C_{21} steroids from the roots of *Cynanchum otophyllum*. *J. Chem. Res.* **2011**, *37*, 126–128. [CrossRef]

33. Abe, F.; Okabe, H.; Yamauchi, T.; Honda, K.; Hayashi, N. Pregnane glycosides from *Marsdenia tomentosa*. *Chem. Pharm. Bull.* **1999**, *47*, 869–875. [CrossRef]

34. Li, X.Y.; Zong, S.L.; Chen, F.Y.; Xu, S.F.; Ye, Y.P. Three novel immunosuppressive steroidal glycosides from the stems of *Stephanotis mucronata*. *Nat. Prod. Commun.* **2012**, *7*, 1269–1270. [CrossRef] [PubMed]

35. Kaur, K.; Khare, M.P.; Khare, A. A novel pregnane ester tetraglycoside from *Orthenthera viminea*. *J. Nat. Prod.* **1985**, *48*, 928–932. [CrossRef]

36. Lee, Y.S.; Kim, W.S.; Kim, K.H.; Yoon, M.J.; Cho, H.J.; Shen, Y.; Ye, J.M.; Lee, C.H.; Oh, W.K.; Kim, C.T.; et al. Berberine, a natural plant product, activates AMP-activated protein kinase with beneficial metabolic effects in diabetic and insulin-resistant states. *Diabetes* **2006**, *55*, 2256–2264. [CrossRef]

37. Zhang, N.; Liu, X.; Zhuang, L.; Liu, X.; Zhao, H.; Shan, Y.; Liu, Z.; Li, F.; Wang, Y.; Fang, J. Berberine decreases insulin resistance in a PCOS rats by improving GLUT4: Dual regulation of the PI3K/AKT and MAPK pathways. *Regul. Toxicol. Pharmacol.* **2020**, *110*, 104544. [CrossRef]

38. Lawson, M.A.; Purslow, P.P. Differentiation of myoblasts in serum-free media: Effects of modified media are cell line-specific. *Cells Tissues Organs.* **2000**, *167*, 130–137. [CrossRef]

39. Zhao, P.; Tian, D.; Song, G.; ming, Q.; Liu, J.; Shen, J.; Liu, Q.H.; Yang, X. Neferine promotes GLUT4 expression and fusio With the plasma membrane to induce glucose uptake in L6 cells. *Front. Pharmacol.* **2019**, *10*, 999. [CrossRef]